MEDICAL SCIENCE MONITOR

LAB/IN VITRO RESEARCH

e-ISSN 1643-3750
© Med Sci Monit, 2019; 25: 2658-2671
DOI: 10.12659/MSM.914269

Received: 2018.11.24
Accepted: 2018.12.12
Published: 2019.04.11

Application of a Strontium-Loaded, Phase-Transited Lysozyme Coating to a Titanium Surface to Enhance Osteogenesis and Osteoimmunomodulation

Authors' Contribution:
Study Design A
Data Collection B
Statistical Analysis C
Data Interpretation D
Manuscript Preparation E
Literature Search F
Funds Collection G

ABCE 1 Xin Lu
BC 1 Wenxin Zhang
BE 1 Zihao Liu
G 1 Shiqing Ma
C 1 Yingchun Sun
G 2 Xudong Wu
AFG 1 Xu Zhang
DG 1 Ping Gao

1 Tianjin Medical University School and Hospital of Stomatology, Tianjin, P.R. China
2 Department of Cell Biology, 2011 Collaborative Innovation Center of Tianjin for Medical Epigenetics, Tianjin Key Laboratory of Medical Epigenetics, Tianjin Medical University, Tianjin, P.R. China

Corresponding Authors: Xu Zhang, e-mail: zhxden@gmail.com, zhangxu@tmu.edu.cn and Ping Gao, e-mail: gaoping@tmu.edu.cn
Source of support: This work was jointly supported by the National Natural Science Foundation of China (NSFC, Grant Nos. 81701019 and 31470919)

Background: To fabricate strontium (Sr)-incorporated titanium (Ti) surfaces by a novel 1-step phase-transited lysozyme (PTL) treatment, and investigate the effects of the prepared samples on osteogenesis and osteoimmunoregulation.

Material/Methods: Five groups of titanium specimens were prepared, including Ti, PTL, PTL@10Sr (PTL coating with 10 mg/mL Sr), PTL@20Sr PTL coating with 20 mg/mL Sr), and PTL@50Sr (PTL coating with 50 mg/mL Sr) groups. Behaviors of bone marrow mesenchymal stem cells (BMSCs) such as initial attachment, spread, proliferation, and migration, on different surfaces were examined by immunofluorescence, MTS assay, and Transwell system. Then the osteogenic differentiation of BMSCs was detected. When an immune response was factored in, the polarization of macrophages induced by the prepared surfaces was detected by real-time PCR, and the response of BMSCs to macrophage-conditioned medium was assessed in terms of cell migration and osteogenic differentiation. Finally, an *in vivo* study was performed, using the rat femora implant model, to evaluate the potential for osteogenic induction and osteoimmunoregulation of materials.

Results: Our *in vitro* experiments indicated that PTL coating could improve cell spread and adhesion, and the stable Sr release of PTL@Sr layers could promote cell migration and osteogenesis. Moreover, PTL@Sr surface could regulate the immune response of macrophages resulting in enhanced BMSCs recruitment and osteogenic differentiation. The *in vivo* evaluation showed less inflammatory infiltration and improved bone formation in the PTL@20Sr group.

Conclusions: The Sr-loaded PTL layers have greater potential for the induction of osteogenic differentiation of BMSCs, meanwhile Sr-loaded PTL layers could adjust the immune response and thus promote osteogenesis both *in vitro* and *in vivo*.

MeSH Keywords: Dental Implantation • Immunomodulation • Osteogenesis • Strontium • Titanium

Full-text PDF: https://www.medscimonit.com/abstract/index/idArt/914269

Indexed in: [Current Contents/Clinical Medicine] [SCI Expanded] [ISI Alerting System] [ISI Journals Master List] [Index Medicus/MEDLINE] [EMBASE/Excerpta Medica] [Chemical Abstracts/CAS]

Background

Titanium (Ti) and its alloys are the most widely used bone-interfacing implant materials in dentistry because of their excellent mechanical properties and superior biocompatibility [1–3]. However, due to the lack of bioactivity and osteoinductivity, a minimum of 3 months is required to achieve sufficient osseointegrated fixation after implantation [4,5]. Many efforts to modify the implant surface have demonstrated that the coating of the implant with bioactive chemical elements could functionalize the surface and accelerate osseointegration [6–8]. Among these elements, strontium (Sr) has similar characteristics to calcium [9,10], which enables Sr to deposit into the mineral phase of bone. Moreover, a series of *in vitro* and *in vivo* experiments and clinical trials have shown that Sr had dual regulatory effects on bone metabolism that could promote osteogenic differentiation to accelerate bone formation and concomitantly suppress osteoclast activation and differentiation to reduce bone resorption [11–13].

The local delivery of an appropriate dose of Sr to the implant-tissue interface has been widely recognized as a promising route for achieving ideal osseointegration [14]. Various techniques, such as micro-arc oxidation, magnetron sputtering, and alkaline heat treatment, have been adopted to manufacture Sr-loaded surfaces for dental implantation; Sr can be directly incorporated into the metal oxide layer or supplemented in the hydroxyapatite coating by substituting for calcium on the Ti surfaces of the implant [15]. However, the production of Sr-modified layers could be costly, employ high voltages (100–1000 V), involve strong alkali treatment, and complicated experimental steps [16–19]. Therefore, these shortcomings necessitate their replacement with a green and efficient method [20,21].

Phase-transited lysozyme (PTL), a stable interfacial modification material proposed by the Yang [22] can bond to surfaces of virtually arbitrary material types or morphologies. Under quasi-physiological conditions, the disulfide bond of native lysozyme can be broken by tris-(2-carboxyethyl)-phosphine (TCEP); this α-helix of lysozyme is then converted into a β-sheet structure, resulting in the formation of an amyloid-like microfiber network that is phase transited [23]. PTL confers positive charges and functional groups such as carboxyl and hydroxyl groups, via a layer-by-layer self-assembly and the introduction of biologically active molecules and ions [24–26]. The proposed 1-step modification reveals a prospective strategy for establishing functional surfaces with green operation and high efficiency.

More recently, accumulating reports have indicated that as a foreign body, an implant can affect the host immune response significantly and the immune system is closely linked with the skeletal system, thereby determining the fate of the implant to some extent [27–29]. Macrophages are highly plastic and closely related to bone homeostasis and thus are often used as model cells to assess the host response to materials. When exposed to implants, macrophages can differentiate into 2 phenotypes: classically activated inflammatory macrophages (M1), which fight infection through the release of pro-inflammatory cytokines; and alternatively activated inflammatory macrophages (M2) encouraging tissue repair and osteogenesis [30,32]. Moreover, studies have found that Sr can regulate the response of macrophages, suppressing interleukin (IL)-6 expression and producing bone morphogenetic protein 2 (BMP2) to promote osteogenesis [33,34]. Thus, an appropriate immune-microenvironment regulated by the designed implants could result in more efficient bone regeneration [35].

Integrating the aforementioned information, we gathered, we prepared Sr-modified titanium surfaces through a novel PTL method and achieved long-term and stable ion release. The released Sr was hypothesized to exert favorable immunomodulatory effects along with its osteogenic effect. To confirm this hypothesis, we implemented systematic studies using *in vitro* biological evaluation and *in vivo* histological experimentation.

Material and Methods

Specimen preparation

The commercial Ti alloy (99.6% purity, Leiden Biomaterials Co., Shanghai, China) was cut into plates and rods (2×2×2 mm). After being polished with silicon carbide (SiC) abrasive paper (grit size starting at #1000, followed by #3000, #5000, and #7000), the Ti plates were ultrasonically cleaned with a sequence of acetone, absolute ethyl alcohol, and deionized water. Then, the substrates were stoved and high-pressure sterilized in an autoclave at 120°C for 30 minutes.

To functionalize the Ti surface with the PTL coating, the substrates were immersed in a mixture containing equal volumes of lysozyme (2 mg/mL, Sigma-Aldrich, St. Louis, MO, USA) 4-(2-hydroxyethyl)-1-piperazineethanesulfonic acid (HEPES) solution (10 mM, Solarbio, Beijing, China), and TCEP (50 mM, Solarbio) HEPES solution (the pH was adjusted to 8 with 1 M NaOH). After 2 hours of incubation at room temperature, the samples were washed extensively with ultrapure water to eliminate residual impurities. The Sr-modified plates were fabricate using Lysozyme HEPES solution containing a certain concentration of Sr (from $SrCl_2 \cdot 6H_2O$): 10 mg/mL, 20 mg/mL, or 50 mg/mL. To improve the release kinetics, we cross-linked PTL with 1-ethyl-3-(3-dimethylaminopropyl)-carbodiimide (EDC, 50 mmol/L, Sigma-Aldrich) and N-hydroxysuccinimide

Indexed in: [Current Contents/Clinical Medicine] [SCI Expanded] [ISI Alerting System] [ISI Journals Master List] [Index Medicus/MEDLINE] [EMBASE/Excerpta Medica] [Chemical Abstracts/CAS]

(NHS, 50 mmol/L, Sigma-Aldrich) aqueous solution. All reaction solutions were sterilized by filtering through 0.2 μm filter membranes.

Depending on the concentration of Sr, the specimens are referred to as PTL, PTL@10Sr, PTL@20Sr, and PTL@50Sr, whereas Ti refers to the pristine specimen.

Surface characterization

The surface morphology of the specimens was characterized by field emission scanning electron microscopy (FE-SEM, Zeiss, Germany). The chemical composition of the uncoated and modified titanium discs was analyzed by x-ray photoelectron spectroscopy (XPS, PHI5000VersaProbe, Japan).

Release of Sr ions

The release of Sr ions from the Sr-modified PTL coating was evaluated by inductively coupled plasma optical emission spectrometer (ICP-OES, Varian725-ES, USA) over a period of 28 days. The samples were submerged in 10 mL of phosphate-buffered saline (PBS). At the relevant time points (1, 3, 5, 7, 14, 21, and 28 days), the total volume of liquid was collected for detection, and replaced by fresh PBS.

Cell culture and osteogenic induction

Rat bone marrow mesenchymal stem cells (BMSCs) (obtained from Beijing University of Chemical Technology, China) and the mouse monocyte/macrophage cell line RAW264.7 (purchased from American Type Culture Collection) were used in the subsequent experiments. Both cell lines were routinely cultured under standard conditions (37°C, 5% CO_2 atmosphere, suitable humidity) in fresh DMEM medium (HyClone, Logan, UT, USA) containing 10% fetal bovine serum (FBS) (Gibco, New York, NY, USA) and 1% penicillin/streptomycin. When the BMSCs reached 80% confluence, the culture medium was replaced with osteoinduction medium supplemented with 50 μg/mL ascorbic acid, 10 nmol/L dexamethasone, and 5 mmol/L β-glycerophosphate. The medium was changed every 2–3 days. The confluent cells were subcultured up to passage 6.

Behavior of BMSCs on the prepared surfaces

Cell adhesion and MTS assay

BMSCs were seeded at a density of 1×10^5/well on the different surfaces in 24-well plates. After 1 hour, 3 hours, and 6 hours of culture, the specimens were submerged in DMEM (without FBS) containing 3-(4,5-dimethylthiazol-2-yl)-5-(3-carboxymethoxyphenyl)-2-(4-sulfophenyl)-2H-tetrazolium (MTS, Promega, Madison, WI, USA) and phenazine methosulfate at a v/v ratio of 100: 20: 1. The supernatants were measured the optical density (OD) at 490 nm to evaluate the relative cell number.

Cell morphology

Cell morphology was observed by immunofluorescence at 6 hours and 24 hours after the cells were inoculated in 24-well plates (5×10^4/well). The samples were fixed in 4% paraformaldehyde and blocked with bovine serum albumin. Finally, FITC-phalloidin (Sigma-Aldrich) was used to visualize the cytoskeleton, and DAPI (Sigma-Aldrich) to stain the cell nuclei. Images were acquired using an inverted fluorescence microscope (Olympus, Tokyo, Japan).

Cell proliferation

The proliferation assay was carried out at the indicated time points (1, 3, 5, and 7 days) using the MTS assay described.

Cell migration

Cell migration experiments were performed via Transwell chambers (Corning, USA). BMSCs were inoculated into the upper chamber with serum-free DMEM. Engineered Ti plates were placed in the lower chamber, and medium containing 10% FBS was added. At 12 hours and 24 hours, the number of cells migrating to the lower chamber was observed by an MTS assay.

Osteogenic differentiation of BMSCs on the prepared surfaces

Cells were seeded on the surfaces in 6-well plates at a density of 1×10^6/well. After 24 hours of cell attachment, the culture medium was replaced by osteoinduction medium.

Alkaline phosphatase (ALP) activity assay

After 7 days and 14 days of culture, the cells were collected, sonicated, and centrifuged to collect the supernatant. Then, the alkaline phosphatase (ALP) content was determined according to the manufacturer's instructions of the ALP kit (NJJ CBIO, Nanjing, China). The ALP levels were normalized to the total protein content as measured by BCA kit (Bio-Rad, CA, USA).

RT-PCR analysis

After incubation with osteoinduction medium for 7 days and 14 days, total cellular RNA was isolated using TRIzol (Gibco). The relative expression of osteogenesis-related genes *osteocalcin (OCN)* and *runt-related transcription factor 2 (Runx2)* was analyzed using *glyceraldehydes-3-phosphate dehydrogenase (GAPDH)* as a control. The primers for these genes are listed in Table 1. The RT-PCR analysis was performed on an Applied

Indexed in: [Current Contents/Clinical Medicine] [SCI Expanded] [ISI Alerting System] [ISI Journals Master List] [Index Medicus/MEDLINE] [EMBASE/Excerpta Medica] [Chemical Abstracts/CAS]

Table 1. Primers sequences used for RT-PCR of BMSCs.

Gene	Forward primer sequence (5'–3')	Reverse primer sequence (5'–3')
RUNX2	GCACCCAGCCCATAATAGA	TTGGAGCAAGGAGAACCC
OCN	GGTGCAGACCTAGCAGACACCA	AGGTAGCGCCGGAGTCTATTCA
ALP	AACGTGGCCAAGAACATCATCA	TGTCCATCTCCAGCCGTGTC
GAPDH	CGTCTTCACCACCATGGAGA	CGGCCATCACGCCAGTTT

RUNX2 – runt-related transcription factor 2; OCN – osteocalcin; ALP – alkaline phosphatase; GAPDH – glyceraldehydes-3-phosphate dehydrogenase.

Table 2. Primers sequences used for RT-PCR of RAW264.7.

Gene	Forward primer sequence (5'–3')	Reverse primer sequence (5'–3')
TNFα	ACTGAACTTCGGGGTGATCG	TGTCTTTGAGATCCATGCCGT
IL-6	CATGTTCTCTGGGAAATCGTGG	TCCAGGTAGCTATGGTACTCC
IL-10	CTCCTAGAGCTGCGGACTG	GCTCCTTGATTTCTGGGCCAT
BMP2	TGCTAGATCTGTACCGCAGG	TCTGTTCCCGGAAGATCTGG
TGFβ1	CAGTACAGCAAGGTCCTTGC	ACGTAGTAGACGATGGGCAG
GAPDH	GGGTCCCAGCTTAGGTTCATC	TGCCGTGAGTGGAGTCATAC

TNFα – tumor necrosis factor α; IL-6 – interleukin-6; IL-10 – interleukin-10; BMP2 – bone morphogenetic protein 2; TGFβ1 – transforming growth factor β1; GAPDH – glyceraldehydes-3-phosphate dehydrogenase.

Biosystems 7500 system using a QuantiTect SYBR Green PCR kit (Qiagen, Hilden, Germany).

Western blotting and immunofluorescence

After 7 days of culture, cells were lysed, and the resulting protein-containing supernatants were transferred to PVDF (polyvinylidene difluoride) membranes. After blocking, the membranes were incubated with anti-Runx2 antibody (1: 1000, Abcam, Cambridge, MA, USA) overnight, followed by incubation with an HRP-conjugated secondary antibody (1: 3000, Abcam) for 2 hours the next day. Targeted protein bands were visualized using an ECL kit (CWBIO, Beijing, China). The intensity of the protein bands was quantified by Adobe Photoshop software.

The general steps for immunofluorescence were described earlier. The primary antibody was an anti-Runx2 antibody (1: 200). The secondary antibody was a rhodamine-conjugated anti-rabbit antibody (1: 200, Invitrogen, Carlsbad, CA, USA). The images were analyzed by Image-Pro Plus software.

Response of macrophages on the prepared surfaces

RAW264.7 were seeded on the engineered surfaces in 6-well plates (1×10^6/well). After 3 days of cultivation, the polarization of RAW264.7 was evaluated by RT-PCR (as described earlier). The primers for the genes involved in this analysis are listed in Table 2.

Response of BMSCs to macrophage-conditioned medium

RAW264.7 cells were cultured on the surfaces (Ti, PTL, and PTL@20Sr) for 1 day, then the medium was collected and mixed with an equal volume of fresh complete DMEM to culture BMSCs.

Cell migration

The migration potential of BMSCs in response to macrophage-conditioned medium was evaluated with Transwell system, as described.

Osteogenic differentiation of BMSCs

BMSCs were cultured in conditioned medium for 7 days and 14 days. The osteogenesis of BMSCs under macrophage co-culture conditions was assessed by an ALP activity assay and RT-PCR analysis, as described.

***In vivo* animal study**

The protocol and procedures employed were ethically reviewed and approved by the Animal Ethical and Welfare Committee.

Indexed in: [Current Contents/Clinical Medicine] [SCI Expanded] [ISI Alerting System] [ISI Journals Master List] [Index Medicus/MEDLINE] [EMBASE/Excerpta Medica] [Chemical Abstracts/CAS]

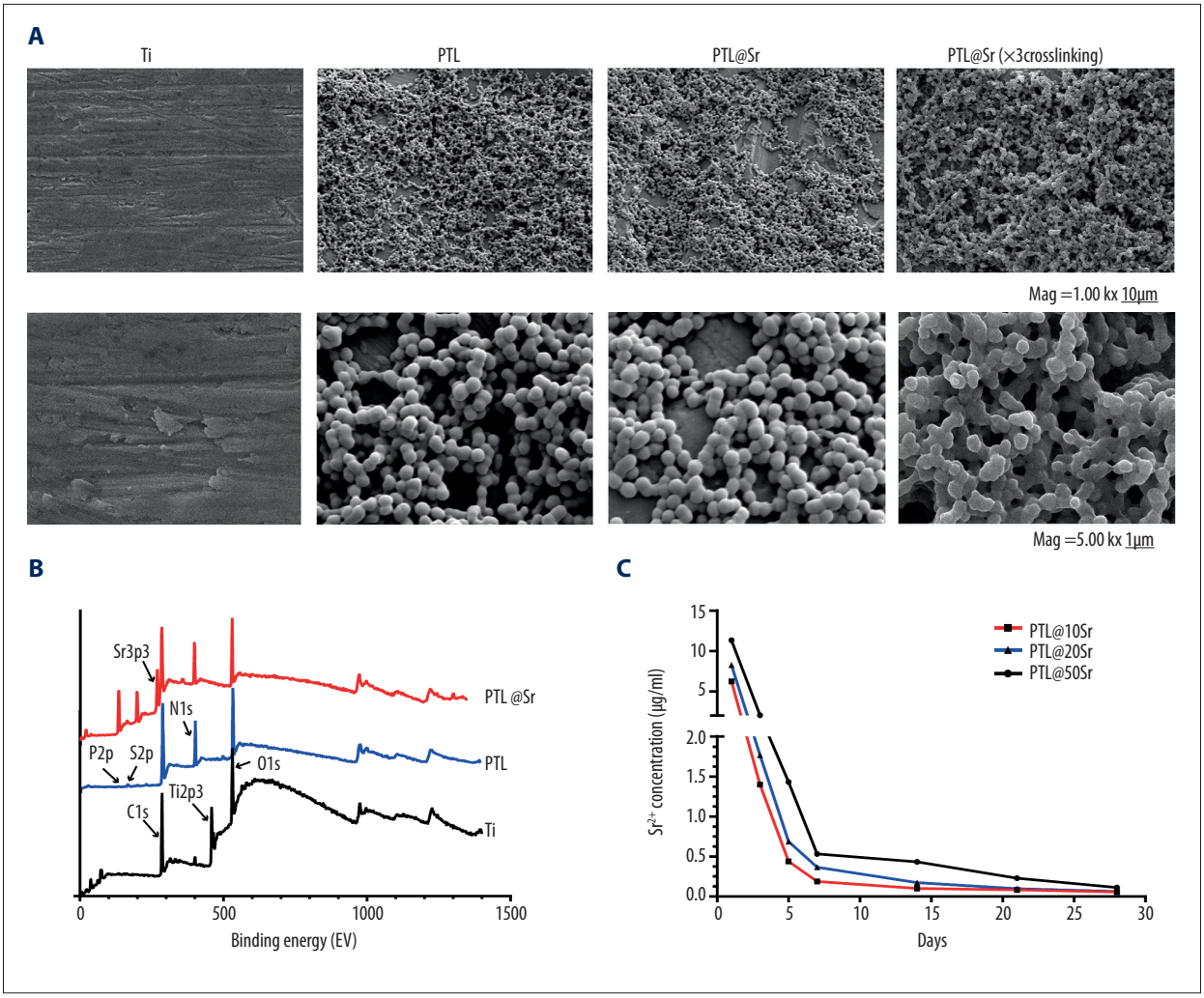

Figure 1. Surface characterization of the prepared samples. (**A**) SEM observation of Ti, PTL and PTL@Sr surface morphologies at 1000× and 5000× magnification. (**B**) XPS survey spectra of Ti, PTL, and PTL@Sr. (**C**) Non-cumulative Sr release curve from PTL@10Sr, PTL@20Sr, and PTL@50Sr, after 1, 3, 7, 14, 21, and 28 days in PBS. SEM – scanning electron microscopy; Ti – titanium; PLT – phase-transited lysozyme; Sr – strontium; XPS – x-ray photoelectron spectroscopy; PBS – phosphate buffered saline.

The femora implant models of 27 Sprague-Dawley rats was established. After 7 days, 9 animals were sacrificed, and the other animals were kept for 4 weeks. The specimens around the implants were fixed, decalcified, embedded in paraffin and sectioned. Immunohistochemistry of CD68 for the 7-day samples and hematoxylin and eosin (H&E) staining for all samples were performed. Undecalcified sections in the 4-week samples were prepared and stained with Van Gieson stain. Analysis of new bone formation was conducted using Image-Pro Plus software in the Van Gieson staining images (magnification 10×).

Statistical analysis

All experiments were repeated at least 3 times to ensure the validity of the evaluation, and the quantitative data are expressed as the mean ± standard deviation (SD). Analysis of statistical significance was performed using one-way ANOVA with a post hoc least significant difference (LSD) test and Student-Newman-Keuls (SNK) test in SPSS 23.0 software. Value of $P<0.05$ was considered to indicate significant difference, and $P<0.01$ highly significant.

Results

Surface characterization

The morphology of the prepared samples was visualized using scanning electron microscopy (SEM). Figure 1A shows that the surface of the Ti plate was flat with some polishing scratches, while the PTL or Sr treated materials exhibited a uniform network structure formed by amyloid microparticles with

Indexed in: [Current Contents/Clinical Medicine] [SCI Expanded] [ISI Alerting System] [ISI Journals Master List] [Index Medicus/MEDLINE] [EMBASE/Excerpta Medica] [Chemical Abstracts/CAS]

Table 3. Atomic concentrations (at.%) on the surfaces determined by XPS.

	C%	N%	O%	Ti%	P%	S%	Sr%
Ti	61.47±0.23	4.64±0.09	26.94±0.12	6.95±0.30	0	0	0
PTL	64.40±0.21	16.28±0.06	18.34±0.20	0	0.16±0.05	0.83±0.07	0
PTL@Sr	58.69±0.37	16.87±0.13	18.19±0.43	0	0.13±0.03	0.81±0.06	5.30±0.03

Ti – titanium surface; PTL – phase-transited lysozyme coating treated titanium surface; PTL@Sr – strontium-loaded phase-transited lysozyme coating treated titanium surface.

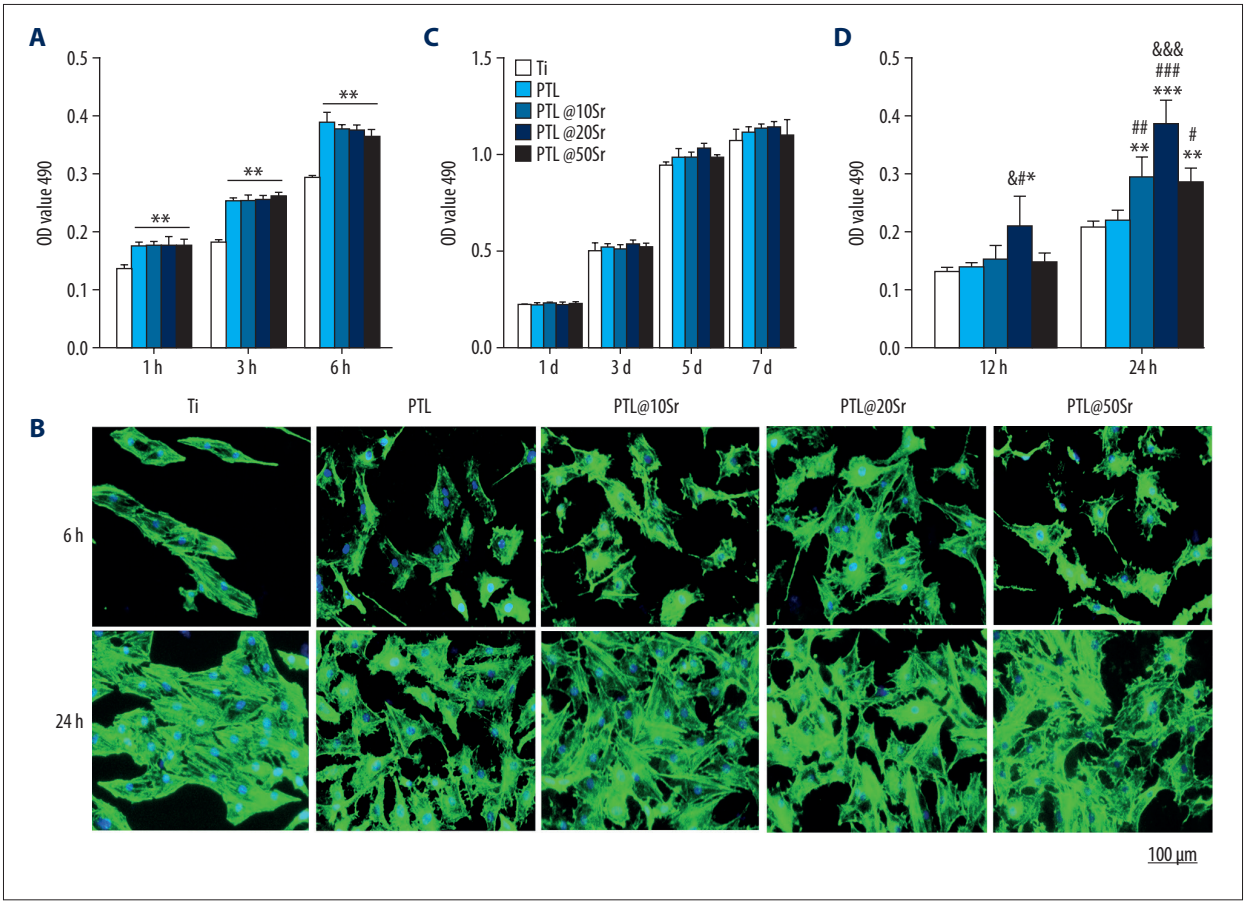

Figure 2. Behavior of BMSCs on the prepared surfaces. (**A**) MTT results of cell adhesion after incubated for 1, 3, and 6 hours on Ti, PTL, PTL@10Sr, PTL@20Sr, and PTL@50Sr surfaces. (**B**) Representative CLSM images of BMSCs (green, cytoskeleton; blue, DAPI) on Ti, PTL, PTL@10Sr, PTL@20Sr, and PTL@50Sr surfaces after 6 hours and 24 hours of seeding. (**C**) Proliferation of BMSCs on Ti, PTL, PTL@10Sr, PTL@20Sr, and PTL@50Sr surfaces. (**D**) Cell migration on different samples examined by Transwell assay. Error bars represent the SD of 3 independent experiments. * $P<0.05$, ** $P<0.01$ compared to Ti; # $P<0.05$, ## $P<0.01$ compared to PTL; & $P<0.05$, && $P<0.01$ compared to PTL@10Sr or PTL@50Sr. BMSCs – bone marrow mesenchymal stem cells; Ti – titanium; PLT – phase-transited lysozyme; Sr – strontium; SD – standard deviation.

a diameter of approximately 500 nm. The chemical composition of the surfaces was assessed by XPS technique, as shown in Figure 1B and Table 3. The appearance of the P and S elements, originating from TCEP and lysozyme respectively, and the disappearance of Ti showed that the Ti substrate was successfully anchored by PTL. The distinctive Sr 3p3 peaks suggested that Sr ions had been deposited in the PTL-modified layer.

Release of Sr ions

Figure 1C shows the Sr release kinetics of the different surface coatings over 28 days. An initial Sr release burst phenomenon was seen for all plates within 1 day, and an equilibrium release period was then achieved after 3 days. The released

Indexed in: [Current Contents/Clinical Medicine] [SCI Expanded] [ISI Alerting System] [ISI Journals Master List] [Index Medicus/MEDLINE] [EMBASE/Excerpta Medica] [Chemical Abstracts/CAS]

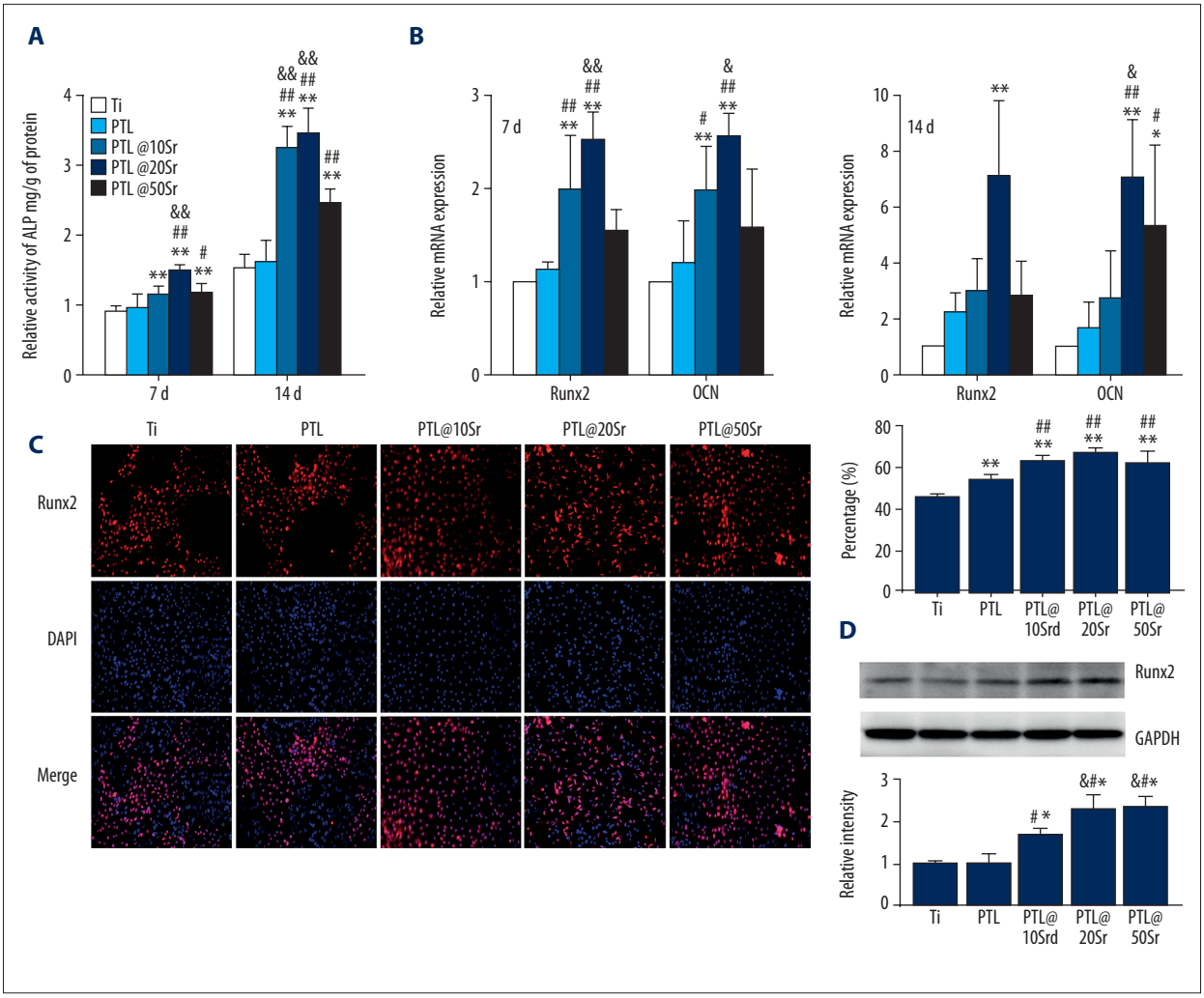

Figure 3. Osteogenic differentiation of BMSCs on the prepared surfaces. (**A**) ALP activity of BMSCs grown on Ti, PTL, PTL@10Sr, PTL@20Sr, and PTL@50Sr surfaces after osteoinduction for 7 days and 14 days. (**B**) The relative mRNA levels of osteogenesis-related genes (*RUNX2*, *OCN*) in BMSCs cultured on different samples for 7 days and 14 days. (**C**) Immunofluorescence staining assays for Runx2 in BMSCs (red, Runx2; blue, DAPI) cultured on different surfaces for 7 days. (**D**) Western blot analysis about the total protein expression of Runx2 in BMSCs at 7 days. Error bars represent the SD of 3 independent experiments. * $P<0.05$, ** $P<0.01$ compared to Ti; # $P<0.05$, ## $P<0.01$ compared to PTL; & $P<0.05$, && $P<0.01$ compared to PTL@10Sr or PTL@50Sr. BMSCs – bone marrow mesenchymal stem cells; ALP – alkaline phosphatase; Ti – titanium; PLT – phase-transited lysozyme; Sr – strontium; SD – standard deviation.

Sr amounts at various time intervals decreased in the order PTL@50Sr >PTL@20Sr >PTL@10Sr.

Behavior of BMSCs on the prepared surfaces

As shown in Figure 2A, the initial cell adhesion was significantly higher on the Sr-modified surfaces, including the PTL-modified surface, than on the Ti surface ($P<0.01$). Interestingly, the numbers of adherent cells on the surfaces treated with Sr and PTL were generally equal. This result indicated that the PTL coating could favor cell adhesion. Regarding the cell morphology (Figure 2B), spindle-like cells could be observed on the Ti surface after 6 hours of culture, while the cells on the other surfaces were extended into polygonal shapes with more obvious pseudopodia. The effects of the different surfaces on cell morphology could endure to 24 hours.

The cell proliferation experiments were displayed in Figure 2C. The MTS activity in BMSCs from all groups increased comparably with time. Treatment with the PTL coatings (with or without Sr) did not induce obvious differences in cell proliferation compared with the Ti counterparts. Figure 2D shows the powerful BMSC-recruiting capacity of Sr-modified surfaces. Moreover, the PTL@20Sr surface exhibited stronger

Indexed in: [Current Contents/Clinical Medicine] [SCI Expanded] [ISI Alerting System] [ISI Journals Master List] [Index Medicus/MEDLINE] [EMBASE/Excerpta Medica] [Chemical Abstracts/CAS]

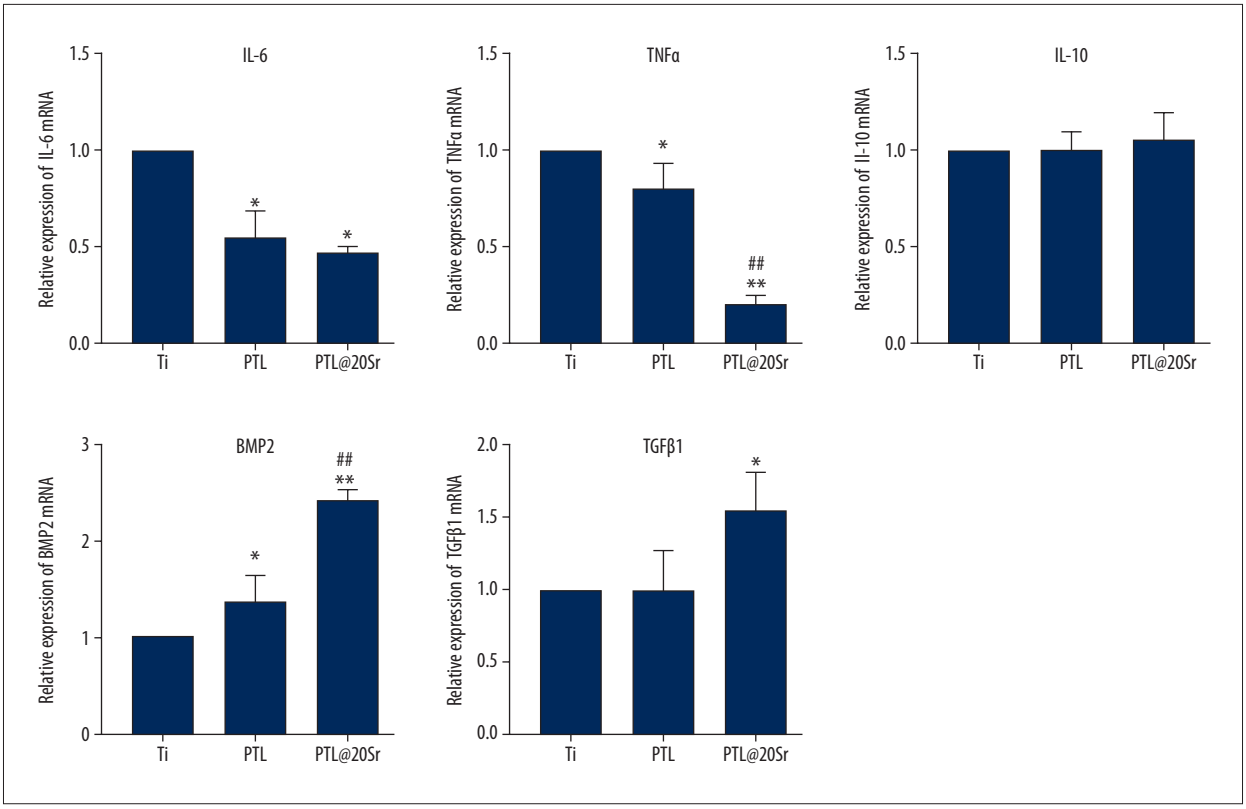

Figure 4. Stimulation of macrophage polarization by the prepared surfaces. The relative mRNA levels of cytokines genes (*TNFα*, *IL-6*, *IL-10*); osteogenic-related genes (*BMP2, TGFβ1*) in RAW264.7 grown on Ti, PTL, and PTL@20Sr surfaces for 3 days. Error bars represent the SD of 3 independent experiments. * $P<0.05$, ** $P<0.01$ compared to Ti; # $P<0.05$, ## $P<0.01$ compared to PTL. Ti – titanium; PLT – phase-transited lysozyme; Sr – strontium; SD – standard deviation.

cell recruitment ability than either the PTL@10Sr or PTL@50Sr surface ($P<0.01$).

Osteogenic differentiation of BMSCs on the prepared surfaces

After 7 days and 14 days of incubation (Figure 3A), the ALP activity levels of the PTL@Sr groups, especially the PTL@20Sr group, were noticeably increased compared with the Ti group and PTL group ($P<0.01$). The RT-PCR results in Figure 3B show that the expression of osteogenesis-related genes *Runx2* and *OCN* were markedly upregulated in the PTL@20Sr group compared with their expression in any of the other groups both at 7 days and 14 days ($P<0.05$). According to the immunofluorescence staining results (Figure 3C), the expression of Runx2 was higher in all PTL groups than in the Ti group and was highest in the PTL@Sr groups ($P<0.01$). The samples enriched in Sr had higher Runx2 expression than the Ti and PTL groups ($P<0.05$), as examined by western blotting (Figure 3D).

Response of macrophages on the prepared surfaces

The results for the response of RAW264.7 (Figure 4) revealed that the expression of the inflammatory gene *IL-6* and *tumor necrosis factor α (TNFα)* were downregulated in cells grown on PTL and PTL@20Sr surfaces compared with the Ti group after culture for 3 days ($P<0.05$). In addition, marked elevation of osteogenesis-related gene *BMP2* and *transforming growth factor β1 (TGFβ1)* expression was found in the PTL@20Sr group compared with the other groups ($P<0.05$), although the expression level of the *IL-10* cytokine gene was not significantly different between the PTL@20Sr group and the Ti group.

Response of BMSCs to macrophage-conditioned medium

As shown in Figure 5A, compared with the control Ti substrate, the macrophage-conditioned PTL and PTL@20Sr samples were more likely to induce cell migration. The results of the ALP activity assay (Figure 5B) showed that cells in the PTL@20Sr group had a higher osteogenic output than cells in the Ti group and the PTL group after culture for 7 days and 14 days ($P<0.01$). Upregulated expression of *RUNX2* (1.88- to 5.38-fold), *OCN* (3.12- to 6.37-fold), and *ALP* (3.52- to 5.48-fold)

Indexed in: [Current Contents/Clinical Medicine] [SCI Expanded] [ISI Alerting System] [ISI Journals Master List] [Index Medicus/MEDLINE] [EMBASE/Excerpta Medica] [Chemical Abstracts/CAS]

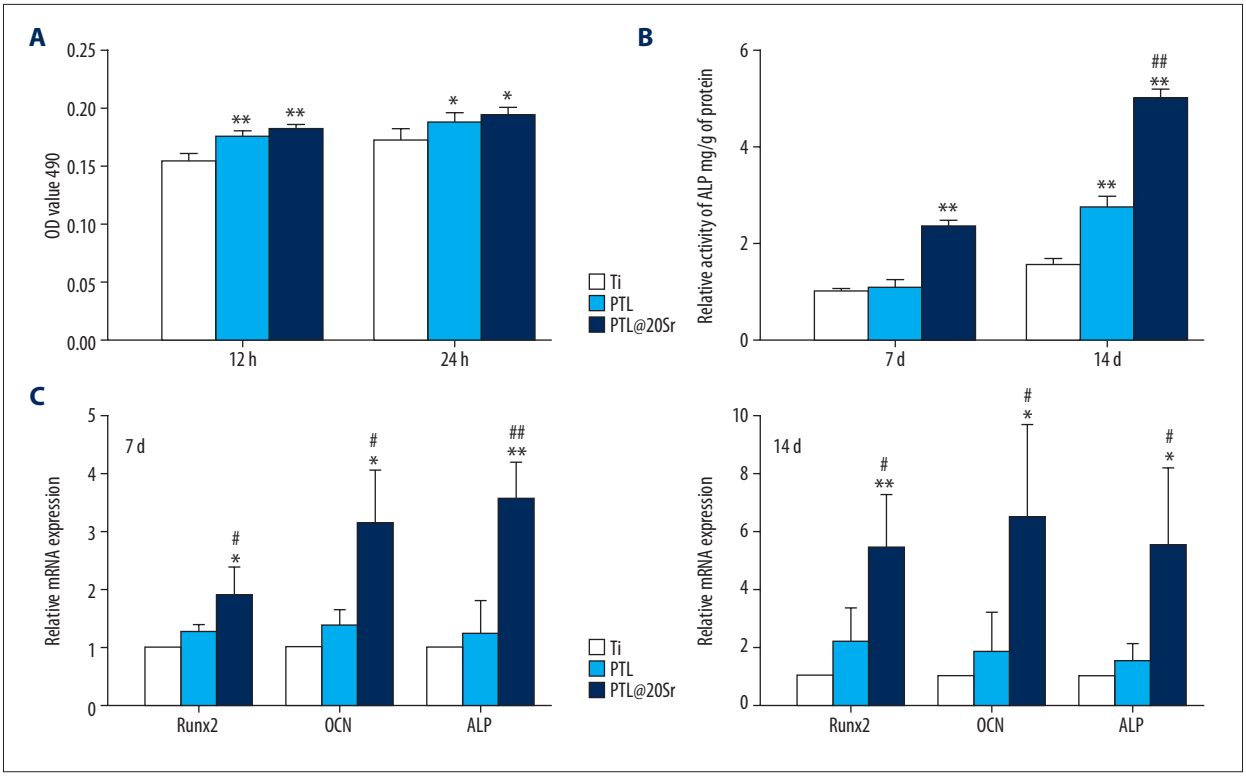

Figure 5. Response of BMSCs to macrophage-conditioned medium. (**A**) Cell migration induced by macrophage-conditioned medium of Ti, PTL, and PTL@20Sr groups. (**B**) ALP activity and (**C**) mRNA expression of osteogenesis-related genes (*RUNX2*, *OCN*, *ALP*) in BMSCs cultured on different groups of macrophage-conditioned medium for 7 days and 14 days. Error bars represent the SD of 3 independent experiments. * $P<0.05$, ** $P<0.01$ compared to Ti; # $P<0.05$, ## $P<0.01$ compared to PTL. BMSCs – bone marrow mesenchymal stem cells; Ti – titanium; PLT – phase-transited lysozyme; Sr – strontium; ALP – alkaline phosphatase; SD – standard deviation.

was observed in the PTL@20Sr group at both 7 days and 14 days ($P<0.05$) (Figure 5C).

In vivo animal study

H&E staining and immunohistochemistry of CD68 were conducted to assess inflammatory infiltration. As shown in Figure 6, lower infiltration of inflammatory cells was seen around the PTL and PTL@20Sr implants compared to the Ti implants. Additionally, there were fewer macrophages (CD68 positive cells) around the PTL@20Sr implants than around the Ti and PTL implants ($P<0.01$), and smaller macrophage distribution in the PTL group than in the Ti group ($P<0.01$). H&E staining and Van Gieson staining were carried out to measure osteogenesis. As shown in Figure 7, a larger amount of new trabecular bone was observed in the PTL@20Sr implant group compared to the Ti samples ($P<0.05$) and the PTL samples ($P<0.05$).

Discussion

This study used a simple and economic strategy with a green reaction process based on PTL to treat the surface of implants with Sr. A stable adhesion between the PTL and the substrates involves complex binding mechanisms, such as metal–sulfur coordination bonding, hydrogen bonding, physical entanglement, and electrostatic and hydrophobic interaction, which can be ascribed to the multiple functional groups exposed on the PTL layer surface [36–38]. A successful combination of Sr and PTL could be explained by the interaction between divalent cations and functional moieties on the PTL surface [39,40]. The stable and enduring release of Sr ions, which could be ascribed to the chelation of Sr and carboxyl groups as well as the crosslinking of the PTL layer, shows that the PTL layer can provide a desirable delivery platform. Therefore, the excellent properties of the PTL layer make this methodology a potential candidate for the surface modification.

To explore the feasibility of this approach for surface modification, the effects of the designed surfaces on cell behavior were evaluated. The recruitment of BMSCs is generally

Indexed in: [Current Contents/Clinical Medicine] [SCI Expanded] [ISI Alerting System] [ISI Journals Master List] [Index Medicus/MEDLINE] [EMBASE/Excerpta Medica] [Chemical Abstracts/CAS]

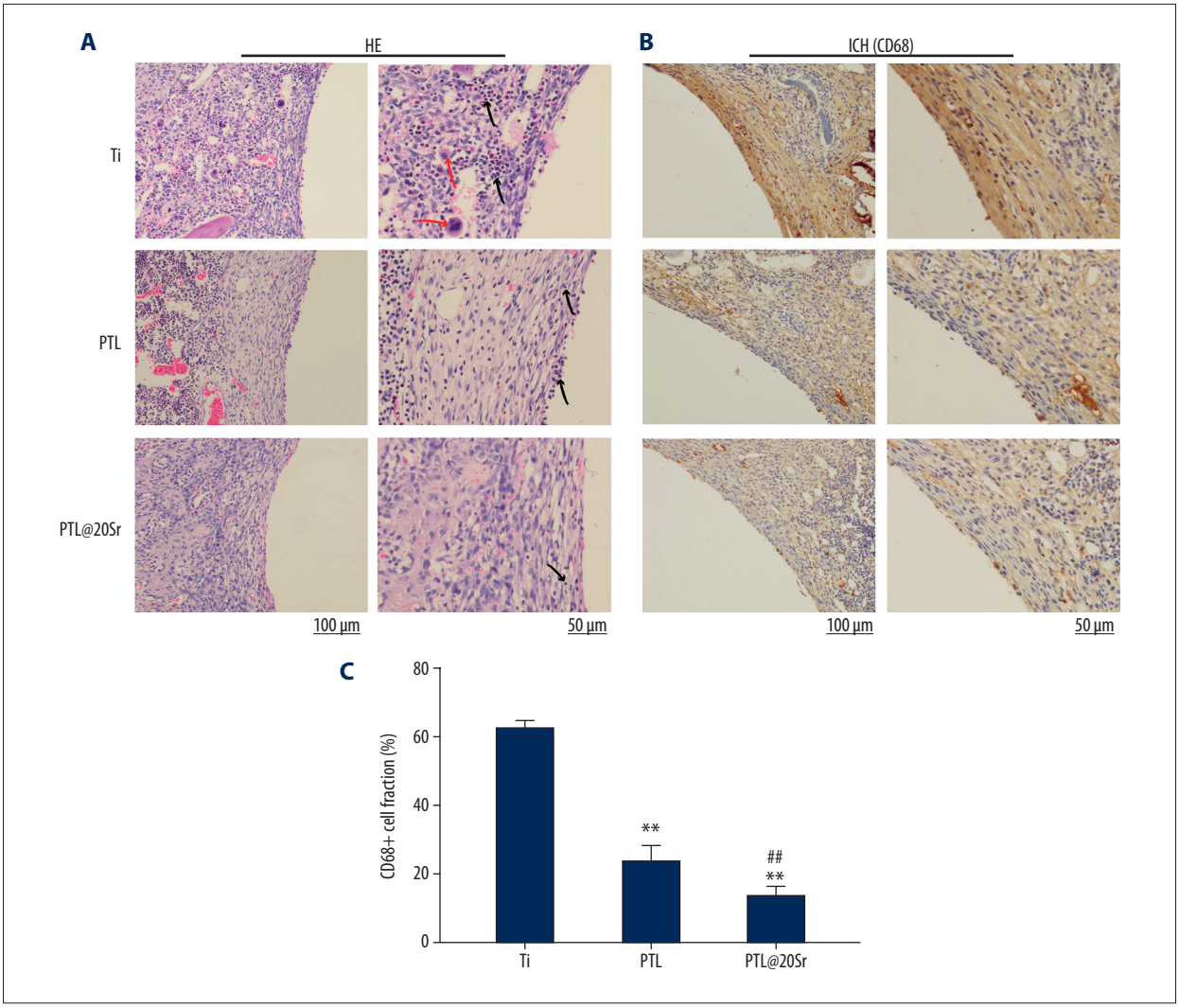

Figure 6. Inflammatory infiltration around the implantation site *in vivo*. (**A**) Hematoxylin and eosin (H&E) staining (black arrows, inflammatory cells; red arrows, multinucleated giant cell) and (**B**) immunohistochemistry of the macrophage marker CD68, 7 days after the implantation of Ti, PTL, and PTL@20Sr titanium specimens. (**C**) Quantitative analysis of $CD68^+$ cell fraction. Error bars represent the SD of 3 independent experiments. ** $P<0.01$ compared to Ti; ## $P<0.01$ compared to PTL. Ti – titanium; PLT – phase-transited lysozyme; Sr – strontium; SD – standard deviation.

believed to play a vital role during osseointegration; after colonizing the implant surface, these cells differentiate into osteoblasts to induce bone growth [41]. Zhou et al. indicated that Sr-incorporated Ti surfaces promote the migration of BMSCs through enhancing the SDF-1α/CXCR4 signaling pathway [42]. In this study, we found that Sr alone increased cell migration across the Transwell membrane and that the PTL layer was not necessary for BMSC chemotaxis.

Initial cell adhesion on biomaterials is a prerequisite for the subsequent growth of cells. After stable adhesion and spreading are established on the surface, the proliferation, differentiation, and maturation of cells ensues [43,44]. As shown in Figure 2, cells on the PTL surfaces exhibited faster adhesion and better extension than those on the Ti surface, probably due to the unique surface characteristics of the modified layers. It is known that cells grow most readily on substrates with similar stiffness. A previous finding indicated that PTL might alter rigid substrates to have a more biocompatible flexible protein interface, which is beneficial to cell attachment [25]. The abundant amyloid microparticles of the PTL layer increases the surface area, thus providing numerous spacing sites for integrin adhesion and resulting in accelerated cell spreading [28,45]. In addition, materials with a positive charge and decoration with -OH, -COOH, and $-NH_2$ functional groups promote cell expansion and adhesion [46]. Thus, the treatment with PTL could improve initial cellular behaviors.

Indexed in: [Current Contents/Clinical Medicine] [SCI Expanded] [ISI Alerting System] [ISI Journals Master List] [Index Medicus/MEDLINE] [EMBASE/Excerpta Medica] [Chemical Abstracts/CAS]

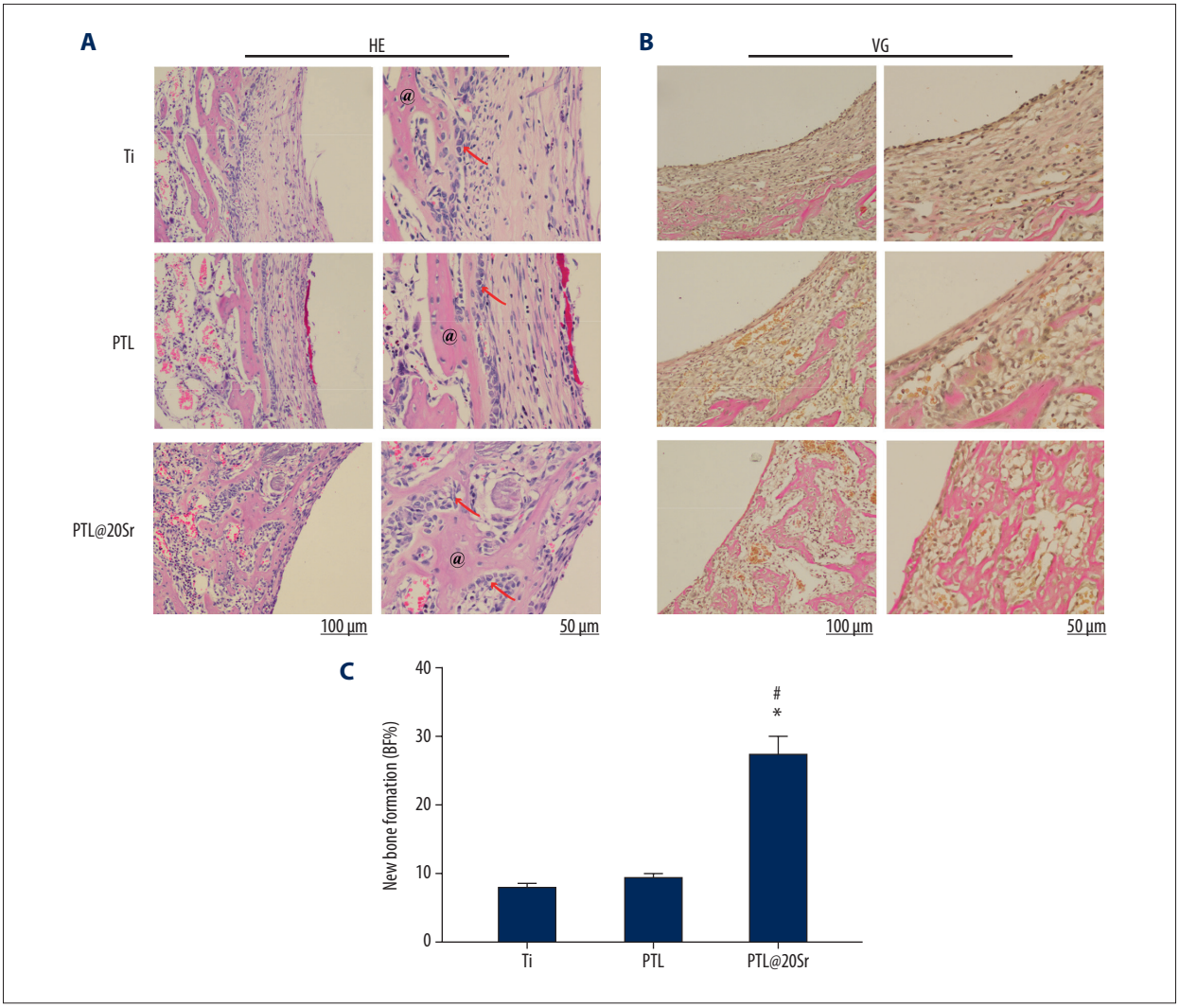

Figure 7. *In vivo* bone formation. Histological samples stained with (**A**) hematoxylin and eosin (H&E) (red arrows, pre-osteoblasts; @, new bone, uniform acidophilic tissue) and (**B**) Van Gieson (staining type I collagen as uniform bright pink), 4 weeks after the implantation of Ti, PTL, and PTL@20Sr Ti specimens. (**C**) Quantitative analysis of new bone formation. Error bars represent the SD of 3 independent experiments. * $P<0.05$ compared to Ti; # $P<0.05$ compared to PTL. Ti – titanium; PLT – phase-transited lysozyme; Sr – strontium; SD – standard deviation.

The available evidence has shown that both PTL and Sr treatments have a negligible effect on cell growth, and is consistent within previous studies [42,47]. However, other research has revealed the promotive effects of Sr on cell proliferation [48,49]. The variation among the different reports might be ascribed to the different cell types and different Sr concentrations and release kinetics in the different studies.

Osteogenesis is indispensable in the process of osseointegration; an array of experiments in this work has provided eloquent proof of the strong effect of Sr and the limited impact of PTL substrate on inducing osteogenic differentiation, in accordance with the findings of previous studies [50,51]. Some studies have revealed that the Sr-mediated activation of canonical and noncanonical Wnt/catenin and Ras/MAPK signaling pathways affects the osteogenic differentiation of mesenchymal stem cells [52,53]. Furthermore, the RANKL-RANK-OPG pathway and the calcium-sensing receptor are responsible for both the progression of bone formation and the inhibition of bone resorption [54–56]. Ni et al. found that the stimulatory effect of Sr on osteoblastic differentiation does not always increase with increasing Sr concentration [57]. Among the samples tested in this study, the PTL@20Sr samples was found to release the most suitable concentration of Sr ions for promoting bone formation.

Among the surfaces, the surfaces with PTL@Sr improved cell activities of adhesion, spreading, migration, and especially

Indexed in: [Current Contents/Clinical Medicine] [SCI Expanded] [ISI Alerting System] [ISI Journals Master List] [Index Medicus/MEDLINE] [EMBASE/Excerpta Medica] [Chemical Abstracts/CAS]

osteogenic differentiation of BMSCs. However, the traditional "one cell type" view does not consider the complex host environment around the implant. It is generally accepted that the earliest event after implant placement is the inflammatory response induced by immune cells, especially macrophages [58,59]. The appropriate response of macrophages could be beneficial to the recruitment of osteoprogenitor cells and the activation of osteogenesis [60]. Therefore, we further explored the osteoimmunomodulation ability of the designed devices.

As shown in Figure 4, the expression levels of proinflammatories of macrophages on the PTL@20Sr samples were lower than that on the PTL or Ti substrate. Macrophages can be activated in different ways by microenvironment, including surface topography and bioactive factors [61]. When activated with the M1 phenotype, macrophages could express and secrete proinflammatory mediators, contributing to the progression of inflammation. By contrast, macrophages polarized to the M2 phenotype have been shown to increase their production of various anti-inflammatory cytokines, resulting in inflammation resolution and wound healing [62,63]. Free Sr ions have been found to regulate the immune status by suppressing TNFα and IL-6 expression in macrophages [64,65]. In this study, the immune response of macrophages might be attributed to the release of Sr in the surface of the PTL@20Sr samples.

Implant-stimulated changes in the inflammatory response directly regulate the homing and differentiation of BMSCs. Additionally, macrophages stimulate BMSC migration through the release of TNFα, IL-6, and so on; in addition, macrophages have been associated with osteogenesis via the secretion of important regulatory molecules such as BMP2 and TGFβ1 [66,67]. Yuan et al. showed that when macrophages are considered, Sr-doped Ti oxides facilitate bone formation [32]. Here, the high level of *BMP2* and *TGFβ1* gene expression stimulated by the PTL@20Sr coating might enhanced osteogenic differentiation, and the suppression of TNFα and IL-6 might have resulted in the improvement of cell migration. Moreover, *in vitro* results confirmed the improved effects of the PTL@20Sr coating on osteogenesis and immunoregulation.

In summary, PTL coating with a certain concentration of Sr was optimal for directly accelerating osteogenesis and promoting bone regeneration by immunoregulation, demonstrating the possibility of designing more effective bone biomaterials through PTL methodology. However, in this study, the interaction between bone cells and immune cells on the surface of the materials was not assessed thoroughly, and the cellular and molecular mechanisms through which strontium affects osteoimmunomodulation are still unclear. These remaining questions will be the focus of our follow-up research.

Conclusions

In this study, Sr was successfully incorporated into a PTL layer on a Ti surface. Sr-loaded PTL coating could regulate the behavior of BMSCs, promoting cell spreading, adhesion and migration, and enhancing osteogenic differentiation. The Sr-loaded PTL coating also invoked greater osteogenesis by affecting the immune environment. The constant *in situ* release of Sr^{2+} ions directly at the implant-tissue interface has been shown to control inflammation and enhance implant osseointegration. Thus, the development of simple and efficient strategies to manufacture implantable materials that incorporate and release bioactive factors to promote osteogenesis and osteoimmunoregulation has great potential to provide new therapeutic options.

Conflict of interest

None.

References:

1. Navarro M, Michiardi A, Castano O, Planell JA: Biomaterials in orthopaedics. J R Soc Interface, 2008; 5: 1137–58
2. Pohler OE: Unalloyed titanium for implants in bone surgery. Injury, 2000; 31: 7–13
3. Liu Z, Ma S, Duan S et al: Modification of titanium substrates with chimeric peptides comprising antimicrobial and titanium-binding motifs connected by linkers to inhibit biofilm formation. ACS Appl Mater Interfaces, 2016; 8: 5124–36
4. Albrektsson T, Zarb G, Worthington P, Eriksson AR: The long-term efficacy of currently used dental implants a review and proposed criterial of success. Int J Oral Maxillofac Implants, 1986; 1: 11–25
5. Oshida Y, Tuna EB, Aktoren O, Gencay K: Dental implant systems. Int J Mol Sci, 2010; 11: 1580–678
6. Wang G, Li J, Zhang W et al: Magnesium ion implantation on a micro/nanostructured titanium surface promotes its bioactivity and osteogenic differentiation function. Int J Nanomedicine, 2014; 9: 2387–98
7. Park JW: Increased bone apposition on a titanium oxide surface incorporating phosphate and strontium. Clin Oral Implants Res, 2011; 22: 230–34
8. Habibovic P, Barralet JE: Bioinorganics and biomaterials: Bone repair. Acta Biomaterialia, 2011; 7: 3013–26
9. Pors Nielsen S: The biological role of strontium. Bone, 2004; 35: 583–88
10. Liu C, Zhang Y, Wang L et al: A strontium-modified titanium surface produced by a new method and its biocompatibility *in vitro*. PLoS One, 2015; 10: e0140669
11. Bonnelye E, Chabadel A, Saltel F, Jurdic P: Dual effect of strontium ranelate: stimulation of osteoblast differentiation and inhibition of osteoclast formation and resorption *in vitro*. Bone, 2008; 42: 129–38
12. Park JW, Kim YJ, Jang JH, Song H: Positive modulation of osteogenesis- and osteoclastogenesis-related gene expression with strontium-containing microstructured Ti implants in rabbit cancellous bone. J Biomed Mater Res A, 2013; 101: 298–306
13. Meunier PJ, Roux C, Seeman E et al: The effects of strontium ranelate on the risk of vertebral fracture in women with postmenopausal osteoporosis. N Engl J Med, 2004; 350: 459–68

Indexed in: [Current Contents/Clinical Medicine] [SCI Expanded] [ISI Alerting System] [ISI Journals Master List] [Index Medicus/MEDLINE] [EMBASE/Excerpta Medica] [Chemical Abstracts/CAS]

14. Xin Y, Jiang J, Huo K et al: Bioactive $SrTiO_3$ nanotube arrays: Strontium delivery platform on Ti-based osteoporotic bone implants. ACS Nano, 2009; 3: 3228–34
15. Shi J, Li Y, Gu Y et al: Effect of titanium implants with strontium incorporation on bone apposition in animal models: A systematic review and meta-analysis. Sci Rep, 2017; 7: 15563
16. Andersen OZ, Offermanns V, Sillassen M et al: Accelerated bone ingrowth by local delivery of strontium from surface functionalized titanium implants. Biomaterials, 2013; 34: 5883–90
17. Zhang W, Cao H, Zhang X et al: A strontium-incorporated nanoporous titanium implant surface for rapid osseointegration. Nanoscale, 2016; 8: 5291–301
18. Liu X, Chu P, Ding C: Surface modification of titanium, titanium alloys, and related materials for biomedical applications. Materials Science and Engineering: Reports, 2004; 47: 49–121
19. Forsgren J, Engqvist H: A novel method for local administration of strontium from implant surfaces. J Mater Sci Mater Med, 2010; 21: 1605–9
20. Guan B, Wang H, Xu R et al: Establishing antibacterial multilayer films on the surface of direct metal laser sintered titanium primed with phase-transited lysozyme. Sci Rep, 2016; 6: 36408
21. Wassmann M, Winkel A, Haak K et al: Influence of quaternization of ammonium on antibacterial activity and cytocompatibility of thin copolymer layers on titanium. J Biomater Sci Polym Ed, 2016; 27: 1507–19
22. Yang P: Direct biomolecule binding on nonfouling surfaces via newly discovered supramolecular self-assembly of lysozyme under physiological conditions. Macromol Biosci, 2012; 12: 1053–59
23. Gao A, Wu Q, Wang D et al: A superhydrophobic surface templated by protein self-assembly and emerging application toward protein crystallization. Adv Mater, 2016; 28: 579–87
24. Zhong X, Song Y, Yang P et al: Titanium surface priming with phase-transited lysozyme to establish a silver nanoparticle-loaded chitosan/hyaluronic acid antibacterial multilayer via layer-by-layer self-assembly. PLoS One, 2016; 11: e0146957
25. Ha Y, Yang J, Tao F et al: Phase-transited lysozyme as a universal route to bioactive hydroxyapatite crystalline film. Advanced Functional Materials, 2018; 28: 1704476
26. Lv H, Chen Z, Yang X et al: Layer-by-layer self-assembly of minocycline-loaded chitosan/alginate multilayer on titanium substrates to inhibit biofilm formation. J Dent, 2014; 42: 1464–72
27. Vi L, Baht GS, Whetstone H et al: Macrophages promote osteoblastic differentiation *in-vivo*: Implications in fracture repair and bone homeostasis. J Bone Miner Res, 2015; 30: 1090–102
28. Bai L, Du Z, Du J et al: A multifaceted coating on titanium dictates osteoimmunomodulation and osteo/angio-genesis towards ameliorative osseointegration. Biomaterials, 2018; 162: 154–69
29. Loi F, Cordova LA, Zhang R et al: The effects of immunomodulation by macrophage subsets on osteogenesis *in vitro*. Stem Cell Res Ther, 2016; 7: 15
30. Brown BN, Londono R, Tottey S et al: Macrophage phenotype as a predictor of constructive remodeling following the implantation of biologically derived surgical mesh materials. Acta Biomater, 2012; 8: 978–87
31. Mosser DM, Edwards JP: Exploring the full spectrum of macrophage activation. Nat Rev Immunol, 2008; 8: 958–69
32. Yuan X, Cao H, Wang J et al: Immunomodulatory effects of calcium and strontium co-doped titanium oxides on osteogenesis. Front Immunol, 2017; 8: 1196
33. Lee CH, Kim YJ, Jang JH, Park JW: Modulating macrophage polarization with divalent cations in nanostructured titanium implant surfaces. Nanotechnology, 2016; 27: 085101
34. Pirraco RP, Reis RL, Marques AP: Effect of monocytes/macrophages on the early osteogenic differentiation of hBMSCs. J Tissue Eng Regen Med, 2013; 7: 392–400
35. Chen Z, Bachhuka A, Wei F et al: Nanotopography-based strategy for the precise manipulation of osteoimmunomodulation in bone regeneration. Nanoscale, 2017; 9: 18129–52
36. Wang D, Ha Y, Gu J et al: 2D Protein supramolecular nanofilm with exceptionally large area and emergent functions. Adv Mater, 2016; 28: 7414–23
37. Wu Z, Yang P: Simple multipurpose surface functionalization by phase transited protein adhesion. Advanced Materials Interfaces, 2015; 2: 1400401
38. Liu R, Zhao J, Han Q et al: One-step assembly of a biomimetic biopolymer coating for particle surface engineering. Adv Mater, 2018; 30: e1802851
39. Yang J, Zhang K, Que K et al: Surface modification of titanium with hydroxyapatite layer induced by phase-transited lysozyme coating. Mater Sci Eng C Mater Biol Appl, 2018; 92: 206–15
40. Yuan N, Jia L, Geng Z et al: The incorporation of strontium in a sodium alginate coating on titanium surfaces for improved biological properties. Biomed Res Int, 2017; 2017: 9867819
41. Tasso R, Fais F, Reverberi D et al: The recruitment of two consecutive and different waves of host stem/progenitor cells during the development of tissue-engineered bone in a murine model. Biomaterials, 2010; 31: 2121–29
42. Zhou C, Xu AT, Wang DD et al: The effects of Sr-incorporated micro/nano rough titanium surface on rBMSC migration and osteogenic differentiation for rapid osteointegration. Biomater Sci, 2018; 6: 1946–61
43. Anselme K: Osteoblast adhesion on biomaterials. Biomaterials, 2000; 21: 667–81
44. McBeath R, Pirone DM, Nelson CM et al: Cell shape, cytoskeletal tension, and RhoA regulate stem cell lineage commitment. Dev Cell, 2004; 6: 483–95
45. Zheng G, Guan B, Hu P et al: Topographical cues of direct metal laser sintering titanium surfaces facilitate osteogenic differentiation of bone marrow mesenchymal stem cells through epigenetic regulation. Cell Prolif, 2018; 51: e12460
46. Li Y, Xiao Y, Liu C: The horizon of materiobiology: A perspective on material-guided cell behaviors and tissue engineering. Chem Rev, 2017; 117: 4376–421
47. Zhang M, Huang X, Hang R et al: Effect of a biomimetic titania mesoporous coating doped with Sr on the osteogenic activity. Mater Sci Eng C Mater Biol Appl, 2018; 91: 153–62
48. Zhao L, Wang H, Huo K et al: The osteogenic activity of strontium loaded titania nanotube arrays on titanium substrates. Biomaterials, 2013; 34: 19–29
49. Chung CJ, Long HY: Systematic strontium substitution in hydroxyapatite coatings on titanium via micro-arc treatment and their osteoblast/osteoclast responses. Acta Biomater, 2011; 7: 4081–87
50. Choudhary S, Halbout P, Alander C et al: Strontium ranelate promotes osteoblastic differentiation and mineralization of murine bone marrow stromal cells: Involvement of prostaglandins. J Bone Miner Res, 2007; 22: 1002–10
51. Kilian KA, Bugarija B, Lahn BT, Mrksich M: Geometric cues for directing the differentiation of mesenchymal stem cells. Proc Natl Acad Sci USA, 2010; 107: 4872–77
52. Peng S, Zhou G, Luk KDK et al: Strontium promotes osteogenic differentiation of mesenchymal stem cells through the RasMAPK signaling pathway. Cell Physiol Biochem, 2009; 23: 165–74
53. Yang F, Yang D, Tu J et al: Strontium enhances osteogenic differentiation of mesenchymal stem cells and *in vivo* bone formation by activating Wnt/catenin signaling. Stem Cells, 2011; 29: 81–91
54. Peng S, Liu XS, Huang S et al: The cross-talk between osteoclasts and osteoblasts in response to strontium treatment: Involvement of osteoprotegerin. Bone, 2011; 49: 1290–98
55. Chattopadhyay N, Quinn SJ, Kifor O et al: The calcium-sensing receptor (CaR) is involved in strontium ranelate-induced osteoblast proliferation. Biochem Pharmacol, 2007; 74: 438–47
56. Hurtel-Lemaire AS, Mentaverri R, Caudrillier A et al: The calcium-sensing receptor is involved in strontium ranelate-induced osteoclast apoptosis. New insights into the associated signaling pathways. J Biol Chem, 2009; 284: 575–84
57. Ni GX, Yao ZP, Huang GT et al: The effect of strontium incorporation in hydroxyapatite on osteoblasts *in vitro*. J Mater Sci Mater Med, 2011; 22: 961–67
58. Gordon S, Taylor PR: Monocyte and macrophage heterogeneity. Nat Rev Immunol, 2005; 5: 953–64
59. Kzhyshkowska J, Gudima A, Riabov V et al: Macrophage responses to implants: Prospects for personalized medicine. J Leukoc Biol, 2015; 98: 953–62
60. Claes L, Recknagel S, Ignatius A: Fracture healing under healthy and inflammatory conditions. Nat Rev Rheumatol, 2012; 8: 133–43
61. Hotchkiss KM, Reddy GB, Hyzy SL et al: Titanium surface characteristics, including topography and wettability, alter macrophage activation. Acta Biomater, 2016; 31: 425–34
62. Brown BN, Ratner BD, Goodman SB et al: Macrophage polarization: An opportunity for improved outcomes in biomaterials and regenerative medicine. Biomaterials, 2012; 33: 3792–802

Indexed in: [Current Contents/Clinical Medicine] [SCI Expanded] [ISI Alerting System] [ISI Journals Master List] [Index Medicus/MEDLINE] [EMBASE/Excerpta Medica] [Chemical Abstracts/CAS]

63. Martinez FO, Helming L, Gordon S: Alternative activation of macrophages: An immunologic functional perspective. Annu Rev Immunol, 2009; 27: 451–83
64. Cardemil C, Elgali I, Xia W et al: Strontium-doped calcium phosphate and hydroxyapatite granules promote different inflammatory and bone remodelling responses in normal and ovariectomised rats. PLoS One, 2013; 8(12): e84932
65. Zhang W, Zhao F, Huang D et al: Strontium-substituted submicrometer bioactive glasses modulate macrophage responses for improved bone regeneration. ACS Appl Mater Interfaces, 2016; 8: 30747–58
66. Chen Z, Yuen J, Crawford R et al: The effect of osteoimmunomodulation on the osteogenic effects of cobalt incorporated beta-tricalcium phosphate. Biomaterials, 2015; 61: 126–38
67. Loi F, Córdova LA, Pajarinen J et al: Inflammation, fraction, bone repair. Bone, 2016; 86: 119–30

Indexed in: [Current Contents/Clinical Medicine] [SCI Expanded] [ISI Alerting System] [ISI Journals Master List] [Index Medicus/MEDLINE] [EMBASE/Excerpta Medica] [Chemical Abstracts/CAS]